

## Supervised classification of water regions from lidar data in the Wadden Sea using a fuzzy logic concept

A. Brzank, C. Heipke

Institute of Photogrammetry and GeoInformation  
University of Hanover  
(brzank, heipke)@ipi.uni-hannover.de

**KEY WORDS:** lidar, laser scanning, classification, fuzzy logic, water

### ABSTRACT:

The Wadden Sea is an almost untouched area with a size of about 7300 km<sup>2</sup> along the German, Dutch and Danish coast. Because of tide the area is flooded two times a day, creating a very special and sensitive ecosystem. In order to protect the Wadden Sea up-to-date Digital Terrain Models (DTM) of high accuracy are needed to detect morphological changes. Lidar is an adequate method to obtain an accurate DTM. However Lidar is not able to penetrate water regions. Thus, raw Lidar data contain several water points, which do not belong to the terrain surface, leading to a wrong DTM.

In this paper we present a supervised classification method to detect water regions from Lidar data using a fuzzy logic concept. Starting with raw data points of one strip, the points are grouped into scan lines. Based on training areas for the classes *water* and *mudflat* the features height, intensity and 2D point density are analysed. The significance level of the assumption that each feature differs for both classes is determined. Then, individual weights are derived from this significance level for every feature taking into account systematic feature changes depending on the angle of incidence of each laser pulse. A fuzzy logic classification is used to distinguish all points into *water* and *mudflat* points. Several additional steps are performed in order to refine and improve the classification result. Two meaningful examples are presented, which show the capability of this supervised fuzzy classification.

### 1. INTRODUCTION

The Wadden Sea is a very special and sensitive ecosystem. Two times a day the area is flooded and falls dry afterwards. The area reaches from Esbjerg, Denmark to Den Helder, Netherlands. Almost 60 % of the 7300 km<sup>2</sup> is situated in Germany. The Wadden Sea represents a unique and protectable wildlife habitat. Many plants and animals have developed in accordance to the tidal influence and their future depends on the existence of the Wadden Sea.

In order to monitor morphologic changes of the Wadden Sea, Digital Terrain Models of high accuracy are needed. Lidar proved to deliver high accurate spatial data of mudflats (e.g. Brzank et al., 2005). However, Lidar is not able to penetrate water. Due to the fact that water still remains in tidal trenches and depressions even during low tide, water points are parts of the captured Lidar data. In order to calculate a DTM, which describes the mudflat surface accurately, water points have to be detected and removed, and additional correct height data have to be introduced.

Depending on the available data sources different approaches are possible. Two general cases can be distinguished. In the first case simultaneous acquisition of Lidar and multispectral image data is assumed. In this case, the images can be used to classify water with standard classification methods. Lecki et al. (2005) pointed out that high-resolution multispectral imagery and appropriate automatic classification techniques offer a viable tool for stream mapping. Within their analysis, especially water was classified accurately. Mundt et al. (2006) demonstrated that the accuracy of classification significantly increases by combining images and height data.

Considering the rapid change of water-covered region caused by a fast changing water level, Lidar and multispectral data has to be captured simultaneously. Taking into account that the flight has to be performed during low tide and the weather conditions must be adequate for multispectral data capturing,

available time windows are rather rare and small. This leads to much higher costs forcing many customers to order only Lidar data. Thus, in the second case, only the Lidar data is assumed to be available. Typically, Lidar data providers deliver irregularly spaced 3D points and intensity values, which correspond to the strength of the backscattered beam echo. Up to now, only a few approaches using exclusively the intensity of Lidar data for classification were published. Katzenbeisser and Kurz (2004) emphasized the fact that classification methods used for remote sensing images need to be adapted to intensity data. They pointed out that the intensity has only a useful information value within open areas where only one echo was detected. Hence, other criteria have to be considered in order to filter water points from Lidar data.

In this paper, we extend the previous approach of Brzank and Heipke (2006). First, we summarize important physical characteristics of Lidar data and previous approaches, which were carried out to separate water and land points in Lidar data. Then, a new supervised method is presented for classification of Lidar data into water and land points.

First, the raw data points are grouped into scan lines. Based on training areas for the classes *water* and *mudflat* the significance of the difference of the features height, intensity and 2D point density is calculated. Then, individual weights are calculated using the significance level for these three features, which also take into account systematic changes of intensity and 2D point density depending on the angle of incidence. Afterwards, a fuzzy classification is performed. All required parameters are obtained from training areas. Finally, the classification result is revised and improved by applying several tests. To illustrate the capability of the algorithm, two examples with different characteristics regarding Lidar scanner system, point density, point distribution etc. are presented. Finally, this paper concludes with a summary and an outlook on further development issues.

## 2. STATE OF THE ART

### 2.1 Physical characteristics of Lidar data within coastal areas

In order to develop a suitable algorithm, which is capable to classify Lidar data (raw 3D Lidar points and their intensity values), the physical characteristics of common Lidar systems as well as the reflection of water and land areas have to be considered. Generally, Lidar systems operate in the near infrared range. Wolfe and Zisis (1989) describe the absorption of infrared radiation depending on the illuminated surface material and the wavelength. They point out that the absorption for water is significantly higher than the absorption for soil. This leads to the fact that the intensity of water points is normally lower than the intensity of land points.

Additionally, as a result of the Rayleigh Criteria, calm water surfaces behave like a mirror. Thus, specular reflection occurs. Often, a distance measurement can not be accomplished successfully because the received radiation energy is not distinguishable from background noise. Hence, the point density of Lidar data within water areas is normally significantly lower than within land areas.

### 2.2 Systematic changes of intensity and point density depending on the angle of incidence

As pointed out in the previous chapter, intensity and point density depend on the characteristics of the illuminated area. The reflectance of water is lower in case of near infrared light than the reflectance of mudflat. However, also mudflat has quite a smooth surface yielding in similar specular reflection behaviour of the laser beam. Thus, intensity and 2D point density are systematically influenced depending on the angle between the laser beam and the surface normal.

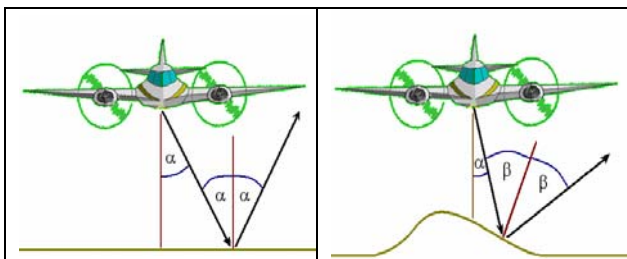


Figure 1. Specular reflection in case of (left) horizontal and (right) tilted area

Figure 1 illustrates how the laser beam is deflected depending on the angle of deflection ( $\alpha$ ) and the angle of incidence ( $\beta$ ), if specular reflection occurs. Assuming that the area of interest is horizontal (which can be stated approximately for large parts of the Wadden Sea)  $\alpha$  equals  $\beta$ . In case of tilted regions the surface orientation has to be taken into account in order to calculate  $\beta$ . Practically, the reflectance behaviour of the laser beam hitting water or mudflat is not exactly equal to specular reflection but similar. Hence, intensity values of points increase, if  $\beta$  decreases. Additionally, more points are measured correctly, if  $\beta$  decreases because the intensity is strong enough to trigger a correct measurement. In order to obtain accurate classification results using intensity and point density, the different reflectance properties of water and mudflat, but also the systematic changes depending on the angle of incidence, have to be taken into account.

### 2.3 Previous approaches to extract water areas from Lidar data

Brockmann and Mandlburger (2001) developed a technique to extract the boundary between land and river water, and applied it to data from the German river "Oder". Based on Lidar data, the planimetric location of the river centre line as well as bathymetric measurements of the riverbed, the boundary was obtained within a two-stage approach. First, the height level of the water area was derived by averaging the Lidar points in the vicinity of the river centre line. Afterwards, a DTM of all Lidar points (including also points of the water surface) was calculated. Then, the 0 m contour line of the difference model of the Lidar DTM and the water height level was derived. This contour line is called "preliminary borderline". Within step two, the bathymetric points of the preliminary water area were combined with all Lidar points outside the preliminary water area. Then, a DTM representing the riverbeds instead of waterlevel was calculated. Afterwards, the final borderline was obtained by intersecting this DTM including the riverbeds and the height level of water area.

Mandlburger (2006) proposed another method based on the same input data, which also detects the borderline of a river. First, the Lidar points are transformed into the river-axis system. Then, segments with a fixed length in flow direction are created. All points for each segment are used to create a profile across flow direction. After removing all outliers (vegetation and water points etc.), bank slopes of both sides are generated by an adjusted line. Then, one border point for each side is calculated by intersecting these lines with the prior known water height. Finally, all border points are transformed back into project coordinate system and linked.

Brzank and Lohmann (2004) (see also Brzank et al., 2005) developed another algorithm which separates water regions from non-water regions based on a DSM calculated from Lidar data. The main idea is to detect reliable water regions and expand those using height and intensity values. For that purpose, local height minima were extracted from the DSM, which represent potential seed zones of water areas. This step was followed by a region growing procedure using height and intensity data of the DSM grid points. In comparison to the previously mentioned algorithms, no additional information, such as water height or river axis is necessary. However, results were not satisfying, because systematic changes of intensity were not modelled.

### 2.4 Fuzzy classification concept

In order to classify water points from Lidar data in the Wadden Sea, the first two concepts described in section 2.3 are not sufficient. The algorithm of Brockmann and Mandlburger (2001) as well as Mandlburger (2006) require additional data, such as water height, approximate position of water and bathymetric data. However, these data are not available for the Wadden Sea. Moreover, the algorithms do not use further available information such as intensity and point distribution. The method of Brzank and Lohmann (2004) is also not sufficient, because systematic changes of intensity are not modelled. Furthermore, the method is not capable of dealing with different water heights within one water region. This remarkable effect occurs, because water height changes over time because of tide. Data of several flight strips are linked together in order to calculate a DSM. The time difference in capturing flight strips can lead to different height levels within one and the same water region.

Hence, Brzank and Heipke (2006) developed a new algorithm which focuses on classifying water points in Wadden Sea using only raw Lidar data. In contrast to previous approaches, classification is carried out for each flight strip separately in order to avoid different water heights within one region. The classification uses a fuzzy logic concept. A membership value for the class *water*  $\mu_i(\underline{x})$  is calculated for every point based on its feature values and their weights. Six different features are used: height, intensity, slope, missed points, segment length and 1D point density. While height and intensity are measured directly for every point, all other features are defined based on points of the same scan line.

The classification is performed for each scan line using a hysteresis threshold method. After classification, several additional routines are performed in order to control and improve the classification result.

Brzank and Heipke (2006) proved that this method is capable to classify water regions. The algorithm has many advantages:

- All feature values can be obtained either directly from the measured point or in connection with other points of the same scan line.
- The classification is carried out for each scan line separately, making the classification very fast.
- The classification is done for every flight strip avoiding height changes due to time differences.
- The classification uses a certain weight for every feature taking into account the individual benefit of this feature for the classification.

However some facts are not taken into account:

- Systematic changes of intensity and point density across the flight direction are not be modelled.
- The needed classification parameters are not derived from data. The user has to set these values.
- The features missed points, segment length and 1D point density refer to one scan line, leading to a more noise depended classification result.
- The features missed points, segment length and 1D point density are correlated, which is not considered in the classification process.

### 3. CLASSIFICATION OF WATER POINTS WITH SUPERVISED FUZZY LOGIC CONCEPT

Based on the evaluation in chapter 2.4, fuzzy classification (Brzank and Heipke, 2006) was improved. First, the number of features was reduced to height, intensity and 2D point density. The features missed points, segment length and 1D point density were replaced by the new feature 2D point density. Thus, for every point the number of Lidar points inside a given polygon is determined. The centre of the polygon is given by the point of interest. Then, the number is divided by the size of the polygon. Furthermore, the feature slope was removed.

In order to tackle systematic changes of intensity and 2D point density their weights depend on the angle of deflection of the measured point. This leads to a new formula to calculate the entire membership value of class *water* (equation 1).

$$\mu(h, i, p, \alpha) = \frac{[\delta_h \mu_h(h) + \delta_i(\alpha) \mu_i(i, \alpha) + \delta_p(\alpha) \mu_p(p, \alpha)]}{[\delta_h + \delta_i(\alpha) + \delta_p(\alpha)]} \quad (1)$$

$h, i, p, \alpha$	individual height, intensity, 2D point density and angle of deflection
$\delta_h, \delta_i(\alpha), \delta_p(\alpha)$	weight for features height, intensity, 2D point density
$\mu_h(h), \mu_i(i, \alpha), \mu_p(p, \alpha)$	membership value water of features height, intensity, 2D point density
$\mu(h, i, p, \alpha)$	entire membership of class water

#### 3.1 Determination of classification parameters from training areas

In order to classify Lidar data into *water* and *mudflat* with the proposed fuzzy logic concept several classification parameters are needed. Table 1 shows these parameters and their function. As pointed out earlier, all parameter are to be derived automatically from training areas.

classification parameter	function
two thresholds to limit the application range of the membership function, (intensity and 2D point density)	transforms crisp height value into fuzzy membership value for height (intensity and 2D point density)
constant weight for height	describes how useful the feature height is evaluated for the selected data set
individual weight for intensity (2D point density)	describes how useful the feature intensity (2D point density) is evaluated for the selected point
water thresholds - low and high	classification of fuzzy membership value of every point into class <i>water</i> or <i>mudflat</i>

Table 1. Classification parameters and their function

First, training areas for the classes *water* and *mudflat* are determined. Typically, prior knowledge is used to define these areas. Then, all Lidar points inside these areas are extracted. Afterwards, the mean height and the corresponding standard deviation for all water and mudflat training areas are calculated. Due to a systematic dependency of intensity and 2D point density on their angle of incidence, the mean values and standard deviations are not significant. Hence, the mean intensity (2D point density respectively) must be referenced either with the angle of incidence  $\beta$  or the angle of deflection  $\alpha$ . For reason of simplicity, we use in this paper only  $\alpha$ . In order to calculate  $\alpha$ , the flight trajectory must be available. Based on the actual position of the plane for each scan line  $\alpha$  can be calculated for every point. If  $\beta$  should be used, the difference between the angle of deflection and the corresponding surface normal must be determined. For this purpose, the DTM is needed. Afterwards, the feature values of intensity and 2D point density of every point can be associated with the corresponding angle. These value pairs are used to fit a monotonically decreasing function for both classes. Generally, every function, which describes the systematic dependency correctly, can be used. We chose a function with 4 parameters (see equation 2), which was formerly used as weight function in linear prediction with robust filtering (Kraus and Pfeifer, 1998).

$$f(r) = \frac{c}{(1 + (ar)^b)} + d \quad (2)$$

Figure 2 shows a typical result of function fitting for intensity of both classes. It can be seen that intensity decreases, if the angle of deflection increases.

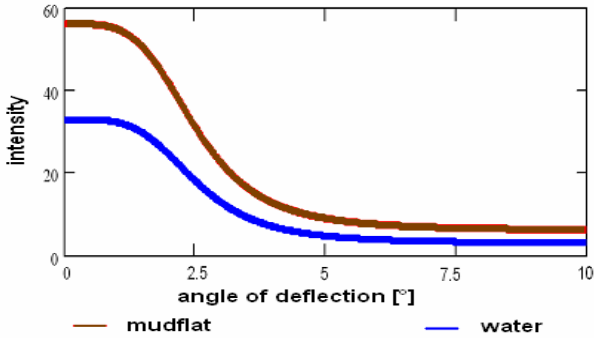


Figure 2. Intensity for both classes as a function of the angle of deflection  $\alpha$

**3.1.1 Determination of membership function and their corresponding thresholds**

In order to transform a crisp feature value into a fuzzy membership value, a membership function and two thresholds, which limit the application area of the membership function, are needed. We define a straight line as membership function. In case of the feature height the determined mean value of class *mudflat* is used as lower threshold with membership value 0, while the mean value of class *water* is used as upper threshold with membership value 1. In case of intensity and 2D point density, the adjusted functions are used. The individual threshold low (high) of every point equals the adjusted value of function *mudflat* (*water*) using the certain angle of the point of interest.

**3.1.2 Determination of individual weights**

In order to calculate the entire membership value of every point individual weights have to be determined. We define the weight to be in the range of 0 up to 1, where 0 means that the feature is not suited and 1 means that the feature is most useful for classification. For the feature height, only one constant weight is determined, because the height values do not depend on the angle of deflection. In case of intensity and 2D point density an individual weight depending on the angle at the point of interest is obtained. In order to calculate the constant weight of the feature height, all training areas for *water* are combined and the mean  $\bar{x}$  and standard deviation  $\bar{s}$  is computed. The training areas of *mudflat* are processed in the same way. Then, the values are used to create the Gaussian distribution of the probability density (Figure 3).

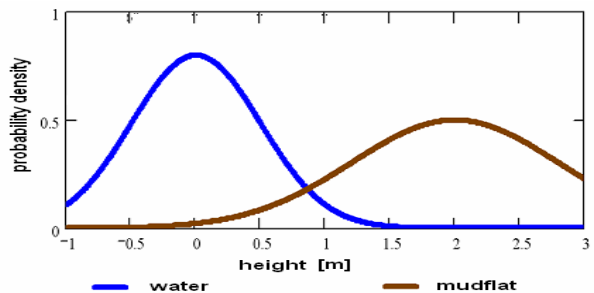


Figure 3. Probability density function of feature height for classes *water* and *mudflat*

It can be stated that the higher the overlapping rate of both distributions the less useful the feature height is to separate between *water* and *mudflat*. Based on this conclusion, the level of significance for the assumption that both distributions are different ( $H_0: \bar{x}_{water} \neq \bar{x}_{mudflat}$ ) is calculated using a statistical test. Equation 3 displays the used test statistics  $t_f$ . Then, the corresponding weight is derived from the level of significance by linear interpolation. For that purpose, two constraints are set. If the level of significance is 50% the weight amounts to 0. In case of 100% the weight is 1.

$$t_f = \frac{\bar{x}_{mudflat} - \bar{x}_{water}}{\sqrt{s_{x_{mudflat}}^2 + s_{x_{water}}^2}} = \frac{d}{s_d} \quad (3)$$

For intensity and 2D point density the determination of the individual weight is very similar. The adjusted values for *mudflat* and *water* are calculated using the estimated features of equation 2. The residuals of all observations of one class are used to calculate the standard deviation. Again, both Gaussian distributions are derived and the level of significance is determined leading to the individual weight depending on the angle of deflection of the point of interest.

**3.1.3 Determination of water thresholds**

After determination of weights the entire membership value of every training point can be calculated using equation 1. Then, the mean of all entire membership values of class *water* and *mudflat* as well as the standard deviation are derived. Now, the two Gaussian distributions of the entire membership value are created. To find the low and high water thresholds the user defines two specific ratios (we normally use 1/10 and 10) of probability density *water* and probability density *mudflat*. The values that match these ratios are used as low and high thresholds.

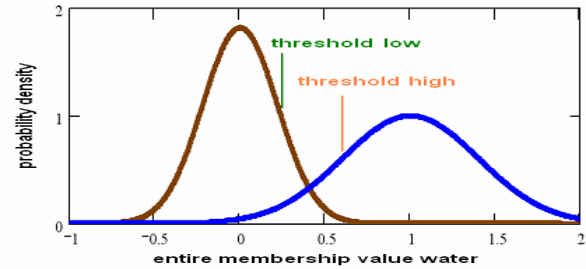


Figure 4. Determination of water threshold low and high

Remark: Generally, a membership value can only lie in the range of 0 to 1. For that reason (see chapter 3.1.1) two thresholds are used in order to limit the use of the membership function. In case of classification all points with feature value below threshold low get a membership value of 0, while all points with feature value above threshold high get a membership value of 1. However, in the analysis of training areas the use of the membership function is not limited leading to membership values below 0 and above 1. This is necessary in order to create normal distributions of the entire membership value *water* (see Figure 4).

**4. EXAMPLES**

In order to demonstrate the ability of the algorithm, two examples are presented in the section. The first example contains a part of a flight strip of the campaign “Friedrichskoog

2005”, which is situated at the coast of the North Sea next to the estuary of the river Elbe. The flight was carried out by the German company Toposys using their Lidar system Falcon II. The second example is a part of a flight strip of the campaign “Juist 2004”. The flight was carried out by German company Topscan using an ALTM2050 from Optech in order to capture Lidar data of the East Friesian island Juist and its surrounding.

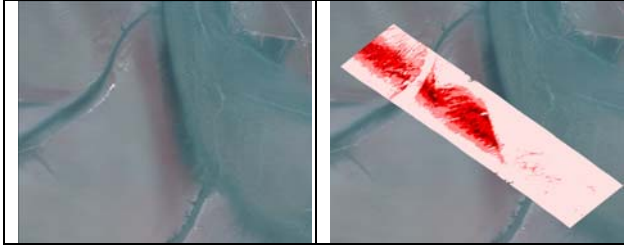


Figure 5. Orthoimage of Lidar campaign “Friedrichskoog 2005” (left) and Lidar points of a part of a flight strip – intensity coded (right)

Figure 5 (left) shows an orthoimage (size: 1.5km length, 1.3km width) of the campaign “Friedrichskoog”. In the image some tidal trenches filled with water as well as a huge water covered swale can be seen. Figure 5 (right) displays captured Lidar points of a part of a flight strip. The points are coded in relation to their intensity (low intensity – bright colour, high intensity – dark colour). It can be seen that the intensity values in the middle of the strip are significantly higher than at the border. Hence, a systematic dependency of the deflection angle exists.

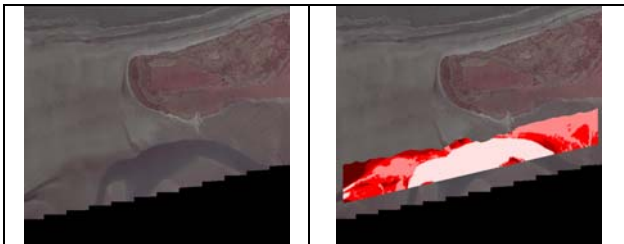


Figure 6. Orthoimage of Lidar campaign “Juist 2004” (left) and Lidar points of a part of a flight strip – intensity coded (right)

Figure 6 displays an orthoimage (size: 4km length, 2.6km width) of campaign “Juist”. There is a huge tidal trench situated south of the island. Again, intensity values are significantly smaller for water than for mudflat. However, a systematic dependency of intensity is not obvious.

Based on the orthoimage a training area for each class was manually selected. Afterwards, all classification parameter were derived from automatic analysis of the training areas. Figure 7 and 8 show the dependency of both classes from angle of deflection for features intensity and point density. The blue (pink) line marks the average feature value of class *water* (*mudflat*), while cyan (ochre) area indicates the single standard deviation of all residuals. As was already obvious from Figure 5, intensity of points from campaign “Friedrichskoog” is systematically influenced by the angle of deflection. Intensity of water and land differ strongly in case of a small angle of deflection. The more the angle increases, the more the intensities for both classes resemble each other. At the border of the flight strip the intensity of water and land do not differ significantly. Hence, the intensity weight within the classification has its maximum for  $\alpha = 0$  and decreases, if  $\alpha$  increases. At the border of the flight strip, intensity is not considered in the classification. In contrast to the intensity, the point density only differs marginally between classes *water* and

*mudflat*. The scan pattern has almost no holes for both training area. Hence, the individual weight of point density is always 0.

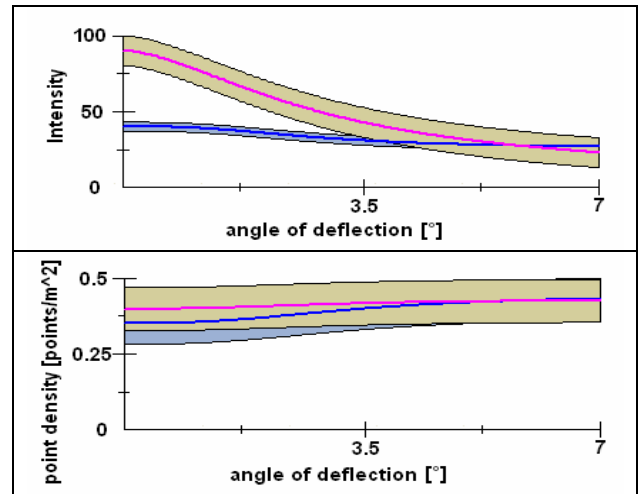


Figure 7. Determination of systematic changes of intensity (up) and point density (down) depending on the angle of deflection - Friedrichskoog

The intensity and point density of Lidar points from the campaign “Juist” only slightly depend on the individual angle of deflection. However, intensity and point density of both classes significantly differ from each other for all angle of deflection. Thus, both features are effective within classification.

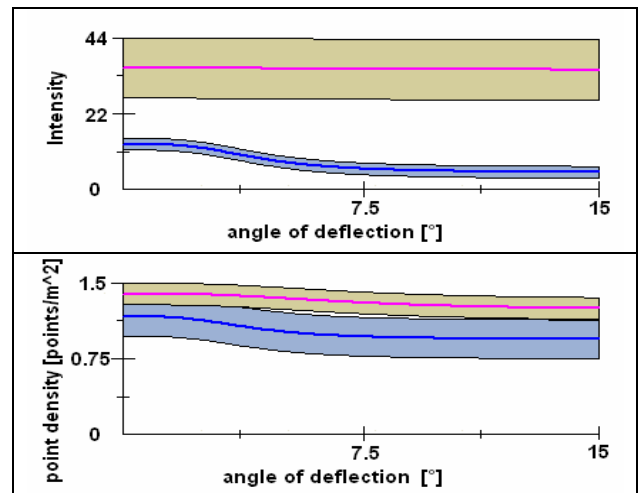


Figure 8. Determination of systematic changes of intensity (up) and point density (down) depending on the angle of deflection - Juist

Based on automatically determined classification parameters, the classification of both datasets was performed. Afterwards, classification discrepancies were detected and removed. Finally, every classification result was smoothed in order to suppress classification noise. Results are displayed in Figure 9 and 10. Figure 9 (left) shows the classification result of campaign “Friedrichskoog”. Based on a visual comparison of the classification result with the orthoimage it can be stated that the overall correctness is satisfying. However, some points within tidal trenches are misclassified due to waves and noisy intensity values. Most highly noisy misclassified points were suppressed by performing additional checks and smoothing leading to the result displayed in Figure 9 (right).

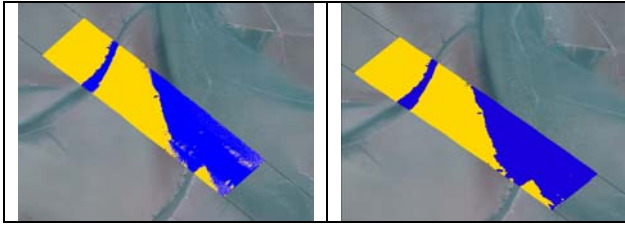


Figure 9. Water (blue) and mudflat (yellow) points after classification (left), additional checks and smoothing (right) - Friedrichskoog

The classification result of campaign “Juist” is visibly slightly better. There are only a few misclassified points due to waves and intensity noise.

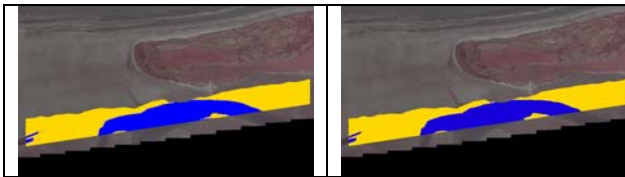


Figure 10. Water and mudflat points after classification (left), additional checks and smoothing (right) – Juist

In order to evaluate the overall correctness, *water* and *mudflat* areas were manually digitized from aerial images and the resulting areas were used as reference for the automatically derived classification. Table 2 lists the results. The correctness of campaign “Juist” is higher than for “Friedrichskoog”. Two reasons can be found. On one side, intensity does not differ significantly for all points while point density is not used for the classification “Friedrichskoog”. In case of “Juist”, all features differ significantly. Furthermore, height increases very slowly at the transition zone from *water* to *mudflat* in case of “Friedrichskoog” making it very difficult to derive correct results. For campaign “Juist” height changes are larger at the transition zone leading to a more accurate classification.

	Friedrichskoog 2005		Juist 2004	
<b>Number of classified points</b>	1.257.518		1.469.405	
<b>Classified water points</b>	592.577		517.858	
<b>Classified land points</b>	664.941		951.547	
	<b>Water</b>	<b>Land</b>	<b>Water</b>	<b>Land</b>
<b>Classified water points</b>	527.641	64.936	510.339	7.519
<b>Classified land points</b>	4.127	660.814	5.886	945.661
<b>Correctness [%]</b>	89.0	99.4	98.5	99.4

Table 2. Evaluated classification results

## 5. CONCLUSION AND OUTLOOK

A supervised fuzzy classification approach to separate Lidar points into the classes *water* and *mudflat* is introduced. The algorithm is based on the original Lidar data and classifies every flight strip. For the analysis the features height, intensity and 2D point density are used. The classification is based on the fuzzy logic concept. All necessary classification parameters are derived from training areas. Two different examples are presented to illustrate the capability of this algorithm. They demonstrate that the classification algorithm is able to deliver accurate results for different Lidar scanner types.

Future work will focus on the determination of highly precise DTMs for the whole investigated areas. For this purpose, bathymetric data has to be included in the calculation in order to fill areas, which are classified as water.

## ACKNOWLEDGMENTS

This research has been financed by the Federal Ministry of Education and Research (BMBF) under project no. 03KIS050. We gratefully acknowledge the support of our project partners: Department of Rural Area Husum (ALR), Federal Waterways Directorate (WSD) and the Lower Saxony Water Management, Coastal Defence and Nature Conservation Agency Division Norden-Norderney (NLWKN).

## REFERENCES

- Brockmann H., Mandlbürger G., 2001. Aufbau eines Digitalen Geländemodells vom Wasserlauf der Grenzoder. In *Publikationen der Deutschen Gesellschaft für Photogrammetrie, Fernerkundung und Geoinformationen*, Band 10, 2001, pp. 199 – 208.
- Brzank, A., Göpfert, J., Lohmann, P., 2005. Aspects of Lidar Processing in Coastal Areas. In *International Archives of Photogrammetry and Remote Sensing*, Hanover, Germany, Vol. XXXVI Part1/W3, CD , 6 p.
- Brzank, A., Lohmann, P., 2004. Steigerung der Genauigkeit von Digitalen Geländemodellen im Küstenbereich aus Laserscannermessungen. In: *Publikationen der Deutschen Gesellschaft für Photogrammetrie, Fernerkundung und Geoinformationen*, Band 13, 2004, pp. 203 – 210.
- Brzank, A., Heipke, C., 2006. Classification of Lidar Data into water and land points in coastal areas. In: *The International Archives of Photogrammetry and Remote Sensing*, Bonn, Germany, Vol. XXXVI/3, pp. 197-202.
- Katzenbeisser, R. and Kurz, S., 2004. Airborne Laser-Scanning, ein Vergleich mit terrestrischer Vermessung und Photogrammetrie. In: *Photogrammetrie Fernerkundung Geoinformation*, Heft 8, 2004, pp. 179-187.
- Kraus K., Pfeifer N., 1998. Determination of terrain models in wooded areas with airborne laser scanner data. In: *ISPRS Journal of Photogrammetry & Remote Sensing*, Volume 53, pp. 193 – 203.
- Leckie, D., Cloney, E., Jay, C. and Paradine, D., 2005. Automated Mapping of Stream Features with High-Resolution Multispectral Imagery: An Example of the Capabilities. In: *Photogrammetric Engineering & Remote Sensing*, Vol. 71, No. 2, February 2005, pp. 145 – 155.
- Mandlbürger, G., 2006. Topographische Modelle für Anwendungen in Hydraulik und Hydrologie. Dissertation, TU Wien. [http://www.ipf.tuwien.ac.at/phdtheses/diss\\_gm\\_06.pdf](http://www.ipf.tuwien.ac.at/phdtheses/diss_gm_06.pdf) (assessed March 29, 2007), 150 p.
- Mundt, J. T., Streutker, D. R., Glenn, N. F., 2006. Mapping Sagebrush Distribution Using Fusion of Hyperspectral and Lidar Classifications. In *Photogrammetric Engineering & Remote Sensing*, Vol. 72, No.1, January 2006, pp. 47 – 54.
- Wolfe, W. and Zissis, G.J. 1989. The infrared handbook. The Infrared Information Analysis Center. Environmental Research Institut of Michigan, Detroit, 1700 p.